THE JOURNAL OF PHYSICAL CHEMISTRY B

Article

pubs.acs.org/JPCB

Structural Transformations, Composition Anomalies and a Dramatic Collapse of Linear Polymer Chains in Dilute Ethanol−Water Mixtures

Saikat Banerjee, Rikhia Ghosh, and Biman Bagchi*

SSCU, Indian Institute of Science, Bangalore 560012, India

Supporting Information

ABSTRACT: Water−ethanol mixtures exhibit many interesting anomalies, such as negative excess partial molar volume of ethanol, excess sound absorption coefficient at low concentrations, and positive deviation from Raoult's law for vapor pressure, to mention a few. These anomalies have been attributed to different, often contradictory origins, but a quantitative understanding is still lacking. We show by computer simulation and theoretical analyses that these anomalies arise from the sudden emergence of a bicontinuous phase that occurs at a relatively low ethanol concentration of $x_{eth} \approx 0.06-0.10$ (that amounts to a volume fraction of 0.17−0.26, which is a significant range!). The bicontinuous phase is formed by aggregation of ethanol molecules, resulting in a weak phase transition whose nature is elucidated. We find that the microheterogeneous structure of the mixture gives rise to a pronounced nonmonotonic composition dependence of local compressibility and nonmonotonic dependence in the peak value of the radial distribution function of ethyl groups. A multidimensional free energy surface of pair association is shown to provide a molecular explanation of the known negative excess partial volume of ethanol in terms of parallel orientation and hence better packing of the ethyl groups in the mixture due to hydrophobic interactions. The energy distribution of the ethanol molecules indicates additional energy decay channels that explain the excess sound attenuation coefficient in aqueous alcohol mixtures. We studied the dependence of the solvation of a linear polymer chain on the composition of the water−ethanol solvent. We find that there is a sudden collapse of the polymer at $x_{eth} \approx 0.05$—a phenomenon which we attribute to the formation of the microheterogeneous structures in the binary mixture at low ethanol concentrations. Together with recent single molecule pulling experiments, these results provide new insight into the behavior of polymer chain and foreign solutes, such as enzymes, in aqueous binary mixtures.

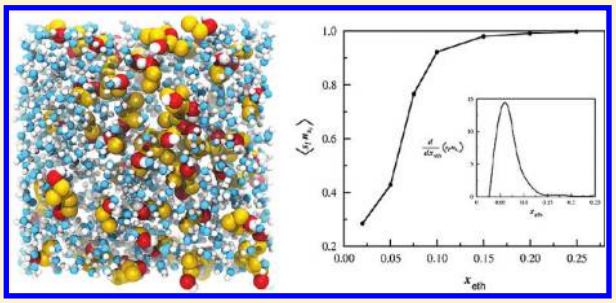

I. INTRODUCTION

Water−alcohol binary mixtures show a range of striking anomalies in several physicochemical properties over a wide range of composition. It is well-known that several thermodynamic and transport properties, like the mean molar volume, diffusion coefficient, compressibility, excess entropy, viscosity, Walden product, sound attenuation coefficient, etc., show significant deviations relative to the ideal solution.[1−6] In most cases, the concentration dependence of these thermodynamic properties shows either maxima or minima in the low alcohol concentration region. For example, the partial molar volumes indicate that the solute apparently contracts up to an alcohol concentration of about 4% for tertiary butanol, 8% for ethanol and 10% for methanol. In their classic review,[1] Franks and Ives interpreted these interesting anomalies in terms of *structural transformations in water−alcohol systems at low concentrations*. They suggested that the nonpolar residues of the alcohol molecules reinforce low entropy water caging, with strong H-bonds in the first hydration shell of the alcohols. This creates an open network structure of water (as in low temperature water or ice). The solute then goes into the open network structure of bulk water, thus reducing the total volume required. This picture, popularly known as the "iceberg" model,[2] received broad support from different studies in the years to follow. Nuclear magnetic resonance studies[7] and molar excess enthalpy measurements[8] generally support this idea. Recent scattering experiments,[9−11] however, introduced a new perspective to this understanding. Soper et al.[12,13] found that there are only minor changes in H-bond occurrence in the first hydration shell of the solute (alcohol), but the major structural change happens in the second hydration shell. The compaction of the second hydration shell was then considered to be responsible for the anomalous behaviors in the dilute alcohol−water solutions. Measurements of the dielectric constant and permittivity spectra[14] offer a different perspective. They suggest competitive self-association of ethanol and water. These measurements indicate formation of microheterogeneous structure of the mixture and existence of precritical concentration fluctuations in the composition range, $0.2 < x_{eth} < 0.4$. This picture has been supported by several other experiments and simulations as well. Mass spectroscopic analysis finds formation of ethanol clusters in the binary mixture, even at a low concentration of 0.07% mole fraction of ethanol.[15]

Received: September 5, 2011
Revised: February 23, 2012
Published: February 24, 2012

   dx.doi.org/10.1021/jp2085439 | J. Phys. Chem. B 2012, 116, 3713−3722

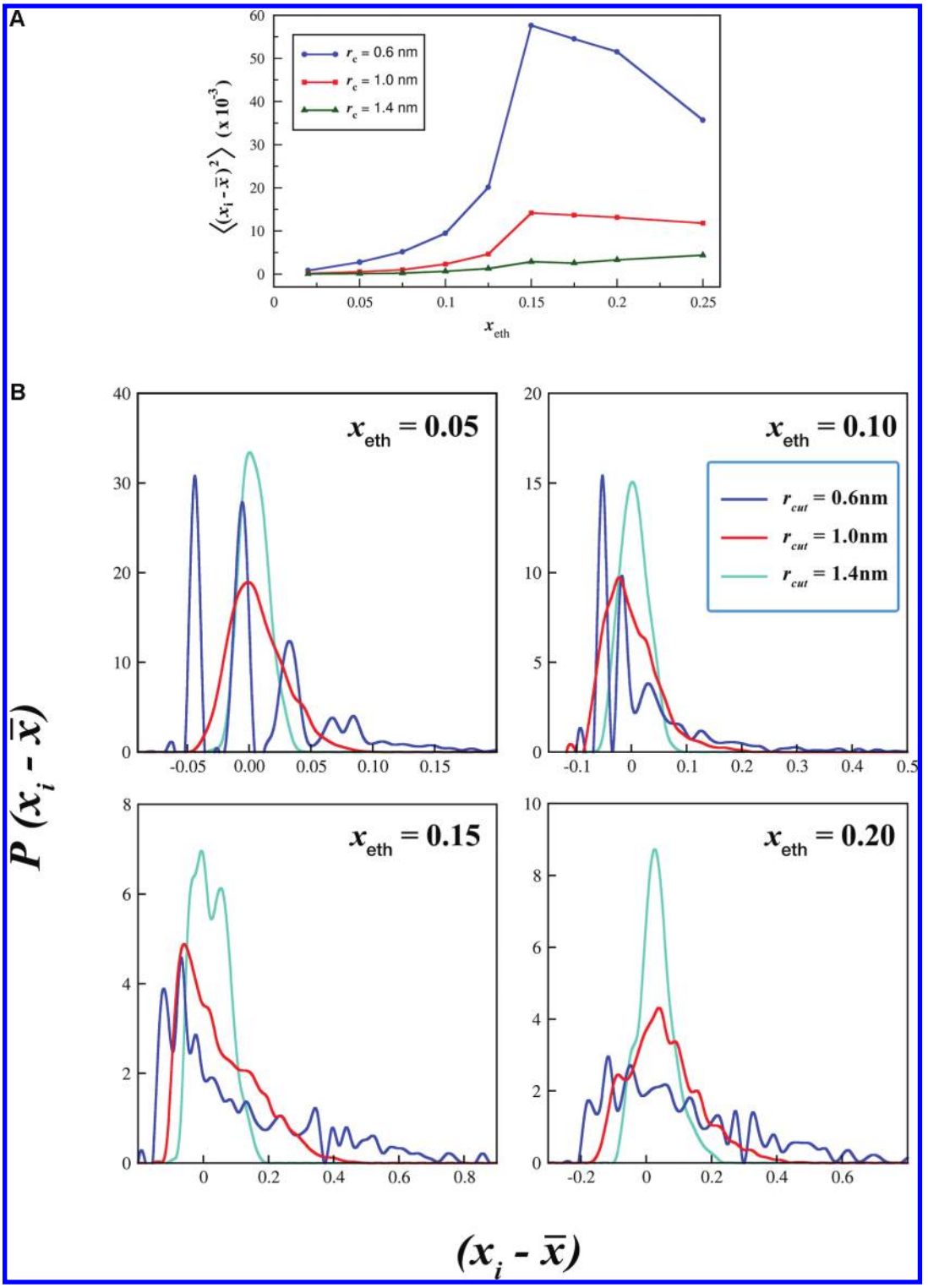

Figure 1. (a) Average local composition fluctuation of the binary mixtures at different concentrations. We consider a sphere of radius r_c and calculate the local composition (ethanol mole fraction, x_i) at every step. The bulk composition of the system is taken as $\bar{x}$, which is same as x_{eth}. We calculate the average local composition fluctuation as $\langle (x_i - \bar{x})^2 \rangle$ at different concentrations of the binary mixture. We note that there is a sharp deviation in the average local composition fluctuation after $x_{eth} \approx 0.10$. The deviation becomes less prominent as we increase r_c, thereby showing that the fluctuation is a local phenomenon. (b) Distribution of composition fluctuation at different concentrations. We consider a sphere of radius r_c and calculate the local composition (ethanol mole fraction, x_i) at every step. The bulk composition of the system is taken as $\bar{x}$. We calculate the probability distribution of $(x_i - \bar{x})$ at different concentrations of the binary mixture and different values of r_c.

Alcohols form H-bonds that lead to their partial or complete solubility in water. The hydrophobic moiety of the alcohols, on the other hand, promotes demixing or segregation by aggregation of alcohol molecules. These two competing factors—segregation and dispersion of the alcohols—makes it a complex problem. As mentioned, numerous experimental and

dx.doi.org/10.1021/jp2085439 | J. Phys. Chem. B 2012, 116, 3713–3722

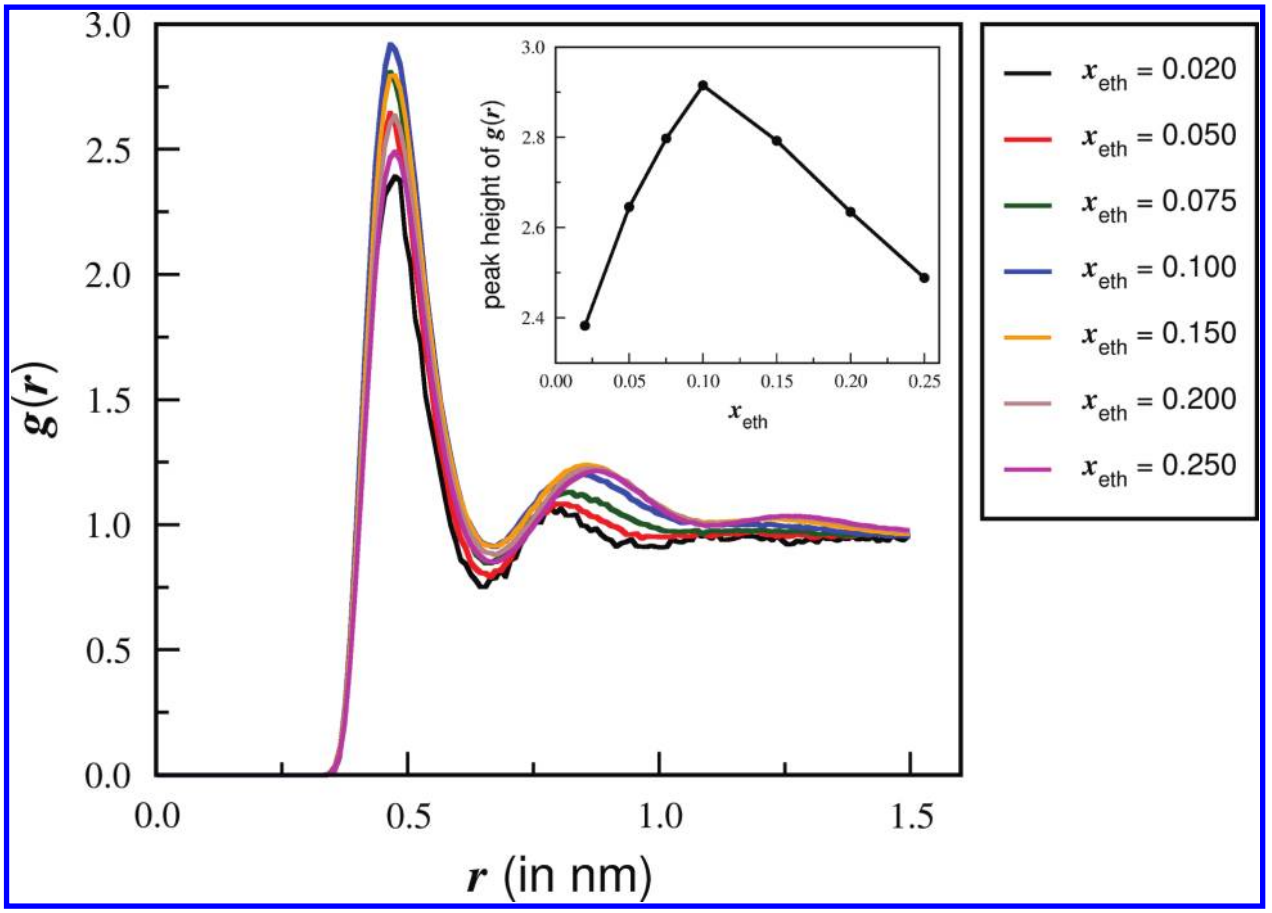

Figure 2. Radial distribution function (rdf) of the ethyl groups at different concentrations of the binary mixture. The legend shows the mole fractions of ethanol at different concentrations. (Inset: the height of the first peak of the rdf at different concentrations).

computer simulation techniques have been applied to study the H-bond network in these mixtures. A recent work[13,16] by Soper et al showed direct evidence of formation of segregated clusters in concentrated water−methanol structure (7:3 molar ratio) by performing neutron diffraction experiments.

However, what remains elusive is an explanation for the existence of extrema and anomalies in a large number of properties at low concentration. Although there have been simulations which reproduce the anomalies at low concentration,[17,18] reason has largely been left unexplored. Theoretical work on binary mixtures is also rare.[19,20]

In this work, we present a quantitative understanding of the anomalies in terms of structural changes that lead to the anomalous behavior in the low concentration limit of water−ethanol binary mixtures. We find that the anomalies arise due to a percolation-like transition leading to the formation of a bicontinuous phase in the binary mixture. It is not surprising that the water persist in a H-bonded cluster at this concentration. An "unexpected" microheterogeneity sets in the system owing to the formation of ethanol clusters at a concentration as low as $x_{eth} \approx 0.06-0.10$. The formation of ethanol clusters is driven by combination of the hydrophobic hydration of the ethyl groups on one hand and the hydrophilic interaction between hydroxyl groups of ethanol and water molecules on the other. The standard approach to percolation yields the threshold at $x_{eth} \approx 0.06$ whereas the calculation of the fractal dimension yields the threshold at $x_{eth} \approx 0.10$.

We have investigated the conformation of a linear polymer chain (with length $n = 30$) in water−ethanol mixture by varying ethanol concentration. In bulk water, the polymer chain exhibits bistability with extended and collapsed state conformations, both almost equally populated. However, near $x_{eth} \approx 0.05$, we find a surprising collapse of the polymer. On increasing the concentration further, the bistability is again restored. We interpret these results in terms of the microheterogeneous structure of the binary mixture.

II. DEPENDENCE OF LOCAL STRUCTURE ON ETHANOL CONCENTRATION

In order to understand the origin of the anomalous behavior of water−ethanol binary mixture we probed the local structure of the system. The origin of the nonmonotonic composition-dependence of many thermophysical properties (like diffusion and viscosity) of binary mixtures can be understood from the composition fluctuation of the system, especially those *at small length scales*.[21,22] Here, we studied the concentration dependence of average composition fluctuation of the system and the radial distribution function of the ethyl groups. In Figure 1a, we show the concentration dependence of the local composition fluctuation (σ_x^2) of the system. We measure the mean square deviation of mole fraction of ethanol in a sphere of a given radius (r_c) at different concentrations of the binary mixture

$$\sigma_x^2 = \langle (x_i - \bar{x})^2 \rangle$$

where x is the mole fraction of ethanol in the mixture. Within a sphere of radius 0.6 nm, we see a sudden increase in the local composition fluctuation after a concentration, $x_{eth} \approx 0.10$.

dx.doi.org/10.1021/jp2085439 | J. Phys. Chem. B 2012, 116, 3713−3722

However, the amplitude of the fluctuation is rather small for larger spherical regions. This is also evident from the distribution of $(x_i - \bar{x})$, as shown in Figure 1b. At small length scales, the distribution is non-Gaussian and we observe fluctuations in the composition of the system. Hence, we have used the variance (σ_x^2), which is related to the second moment of the distribution, to quantify the fluctuations. As we increase the length scale, the distribution becomes less fluctuating. These results indicate that there is a microheterogeneity in the system, and also there is a sudden change in the local structure of the binary mixture after a concentration, $x_{eth} \approx 0.10$. This abrupt behavior in local composition fluctuation motivated us to study further details of the local structure of the system. We anticipated the formation of interesting structures in the system. The implications of this result will be discussed later after we gain more insight into the structure of the binary mixture.

In Figure 2, we show the radial distribution function (rdf) of the ethyl groups at various concentrations of the mixture. We consider a dummy atom at the center of mass of the CH_3 and CH_2 groups, and calculate the rdf of those dummy atoms. We see that the height of the first peak of the rdf increases up to $x_{eth} \approx 0.10$, but then starts decreasing. The change in height of the first peak at various concentration of the binary mixture has been shown in the inset. The first minima of the rdf plots gives us a measure of the coordination shell. With this prior knowledge of the coordination shell, 0.64 nm, we will define the ethanol clusters in the following section and discuss the standard approach of percolation theory.

III. CLUSTERING OF ETHANOL MOLECULES: FORMATION OF THE BICONTINUOUS PHASE

It has been confirmed that liquid water is characterized by the existence of an extensive interconnected network of hydrogen bonds that percolates through the entire phase.[23,24] Pure water reveals a H-bonding network extending over the whole liquid, and only 1% of the H-bonds are not connected to the bulk H-bond network.[25] In case of aqueous binary mixtures, as we increase the concentration of the nonaqueous solute, the H-bond networking starts becoming less dense, and larger disconnected clusters begin to be observed. It has been claimed in previous studies, that the critical percolation point of the water network appears to be at $x_{eth} \approx 0.50$[18] (for water−ethanol mixture) and $x_{meth} \approx 0.54$[13,25] (for water−methanol mixture). In our study, we have focused on the low concentration regime of the water−ethanol binary mixture, and throughout this range the H-bonded network of water remains above the percolation threshold. However, the formation of clusters of the nonaqueous solute was not studied in great detail, and here we report some interesting observations of the cluster analysis of ethanol molecules. We had previously shown in our study[26,27] of water−dimethyl sulfoxide (DMSO) binary mixture that the percolation transition of the network of hydrophobic methyl groups in DMSO leads to the formation of a bicontinuous phase and anomalous behavior of the mixture. In our present study also, we find that the ethyl groups of the ethanol molecules start forming a network as we increase the concentration of ethanol in the binary mixture, and finally forms a percolating network.

For the cluster analysis of the hydrophobic ethyl groups, we consider dummy atoms at the center of mass of the CH_3 and CH_2 groups of ethanol. These dummy atoms serve as the building blocks of the network. If two units are closer than a distance of 0.64 nm (note that this is the distance at which the first minima appears in the rdf, Figure 2), we consider them to be connected. A cluster is defined as a group of these dummy atoms connected by the nearest-neighbor distance. We calculate the basic quantities involved in percolation,[28] i.e., s and n_s. The size of the cluster is s, and n_s is the average number of s-clusters per ethanol group. Figure 3 shows the plot of sn_s at

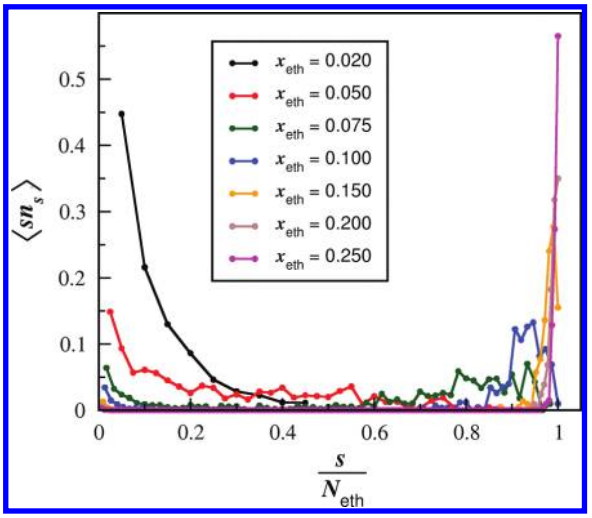

Figure 3. Plot of sn_s against s/N_{eth} at various concentrations of water−ethanol binary mixture. The size of the cluster is s, n_s is the average number of s-clusters per ethanol group, N_{eth} is the total number of ethanol molecules in the system (at that particular concentration) and x_{eth} is the mole fraction of ethanol in the binary mixture. At lower concentrations, we find that the clusters of smaller sizes dominate. Large clusters start appearing from $x_{eth} \approx 0.075$. The largest cluster gradually becomes dominating at higher concentration.

various concentrations of the binary mixture. We note here that clusters of several sizes are prevalent in the mixture at low ethanol concentrations, but at relatively higher ethanol concentration, a continuous large cluster dominates. This indicates that there might be a percolation transition of the ethanol clusters.

The formation of a percolating network demands an explicit detection of the percolation threshold. Therefore, we define an order parameter for the transition as $\langle s_l n_{s_l} \rangle$, where s_l is the size of the largest cluster, n_{s_l} is the number of largest clusters per ethanol group, and the $\langle ... \rangle$ denotes the average over the timesteps. At lower concentrations of ethanol, there might be more than one cluster with the largest size. As we increase the concentration, the value of n_{s_l} becomes $1/N_{eth}$, since only one largest cluster prevails in the system. It is obvious that the value of the order parameter approaches zero as we move toward the limit $x_{eth} \to 0$, and the value approaches 1, as we move toward the limit $x_{eth} \to 1$. The plot of the order parameter in Figure 4 shows a point of inflection, and the derivative plot (shown in the inset) clearly shows that the transition takes place at $x_{eth} \approx 0.06$.

As discussed by Stauffer,[28] the percolation threshold is also evident from the plot of $\sum s^2 n_s$. Therefore, we plot the second moment of s normalized by the total number of ethyl groups, i.e., $(\sum s^2 n_s)/N_{eth}$ at various concentrations of the binary mixture. Here, N_{eth} is the total number of ethyl groups ("dummy atoms" of our cluster) present in the system. The second moment is, in effect, a susceptibility term. In analogy with the standard approach of percolation theory, the different

dx.doi.org/10.1021/jp2085439 | J. Phys. Chem. B 2012, 116, 3713−3722

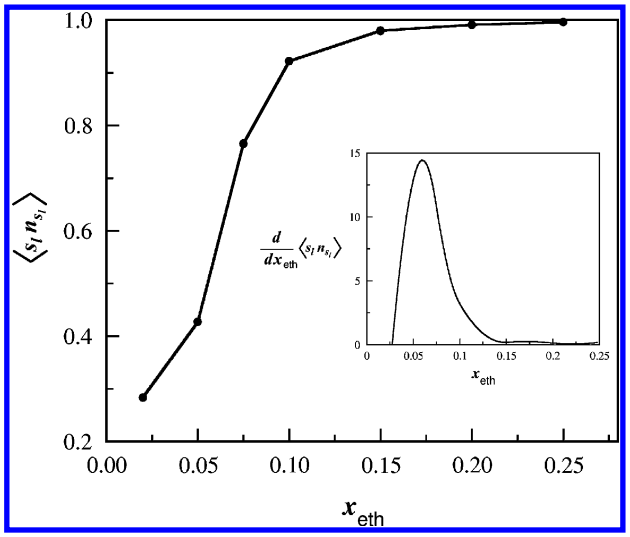

Figure 4. Plot of the order parameter, $\langle s_l n_{s_l} \rangle$ against mole fraction of ethanol (x_{eth}) at different concentrations of the water−ethanol binary mixture. s_l is the size of the largest cluster, n_{s_l} is the number of largest clusters per ethanol group, and the $\langle\rangle$ denotes the average over the timesteps. We show the derivative of the *fitted* plot in the inset (the fit is not shown here). It shows that the maximum appears at $x_{eth} \approx 0.06$.

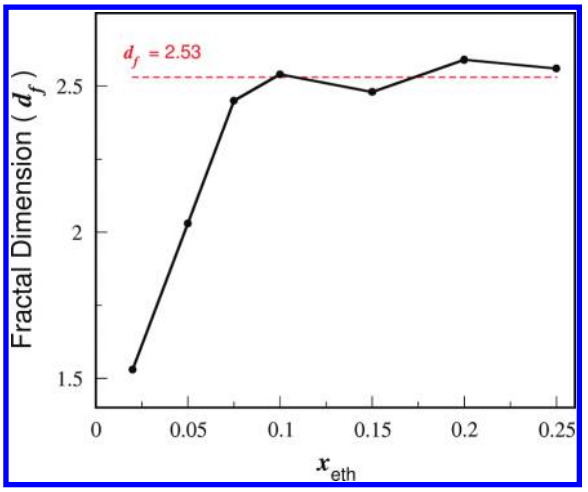

Figure 5. Fractal dimension, d_f of the largest cluster in the system at different concentrations of the binary mixture. As noted previously, x_{eth} is the mole fraction of ethanol in the binary mixture. It has been already established before that the percolation threshold for a cluster in a three-dimensional system is located where the fractal dimension of the largest cluster reaches the critical value of 2.53. The red dotted line shows the critical value, d_f = 2.53. We note that, according to this definition, the percolation threshold for ethanol in the water−ethanol binary mixture appears at $x_{eth} \approx 0.10$.

concentrations of the binary mixture represent the different occupational probabilities. The summation has been done over all available cluster size s in the system. This plot has been shown in the Supporting Information, Figure SI1. The derivative plot (shown in inset) depicts a clear divergence of susceptibility at around $x_{eth} \approx 0.06$.

IV. ANALYSIS OF PERCOLATION THRESHOLD USING FRACTAL DIMENSION

The cluster analysis as discussed above predicts a percolation transition at $x_{eth} \approx 0.06$. To substantiate our findings, we have also calculated the fractal dimension of the largest cluster at various concentrations of the binary mixture. It has been argued before[29,30] that *the largest cluster of a system is a fractal object above the percolation threshold and no objects with fractal dimension lower than 2.53 can be infinite in three-dimensional space. Hence, the true percolation threshold is located where the fractal dimension of the largest cluster in the system reaches the critical value of 2.53.*

The fractal dimension of the largest cluster has been evaluated using the sandbox method. The key idea is to measure from a chosen point of the largest cluster of the system, how many other points lie within a given radius. In effect, however, this gives the cumulative radial distribution function of the groups belonging to the largest cluster of the system, as shown in Figure SI2, Supporting Information. We denote this function as $m(r)$. In other words, $m(r)$ is the number of groups belonging to the largest cluster and are located closer than the distance r from the center of mass of the cluster. The fractal dimension, d_f is then evaluated by fitting the following equation:

$$m(r) \sim r^{d_f}$$

We obtained the values of fractal dimension from the logarithmic plot (not shown here). In Figure 5, we show the plot of the fractal dimensions, d_f at various concentrations of ethanol in the binary mixture. We find that the fractal dimension just reaches the critical value at $x_{eth} \approx 0.10$. While this proves that for the water−ethanol binary mixture, the ethyl groups form a percolating network, the percolation clusters appear to be "flickering". The percolation threshold as measured by standard approach and that from the fractal dimension are in close agreement, and we would, therefore, like to safely conclude that the threshold appears somewhere in the region $x_{eth} \approx 0.06$−0.10.

This phase-transition-like behavior is also implied by the composition fluctuation of the system. In Figure 1, we note that the composition fluctuation increases abruptly after $x_{eth} \approx 0.10$. The percolation transition, as is now evident, leads to a bicontinuous phase of ethanol and water. We believe that at the transition point, there is a dynamic equilibrium between the "clustered" ethanol molecules and the "free" ethanol molecules in the system. This is reflected in the local composition fluctuation of the system.

V. NEGATIVE PARTIAL MOLAR VOLUME OF ETHANOL: EFFICIENT PACKING OF THE ETHANOL MOLECULES IN AGGREGATION

It is generally accepted that the ethanol molecules form an almost-parallel alignment in gas-phase dimers,[31] owing to the formation of H-bonds. Detailed studies have been done on gas phase conformation of ethanol molecules, all showing arrangements with parallel alignment of the ethyl groups in the dimer. However, the conformation of the ethyl groups in aqueous binary mixture has not been looked into. We looked into the angular distribution of the ethyl groups within a given cluster. We considered all ethyl groups, whose center-of-mass lies within 0.64 nm of the central ethyl group, to be the neighbors (note that we used the same definition for the cluster formation). We calculated the angles between the central ethyl group and its neighbors and plotted the distribution of the cosine of those angles in Figure 6. This gives us a probability density of the angular orientation of the ethyl groups. As

dx.doi.org/10.1021/jp2085439 | J. Phys. Chem. B 2012, 116, 3713−3722

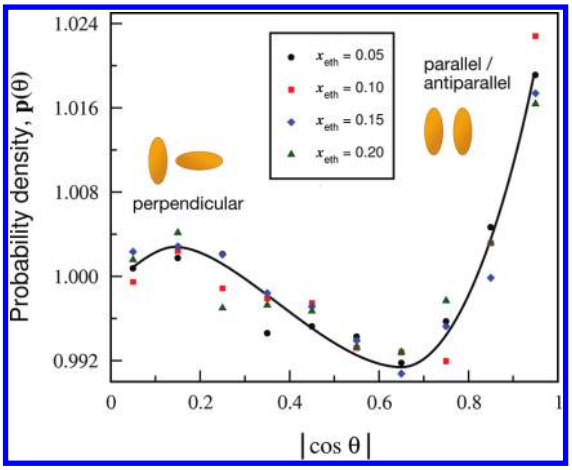

Figure 6. Plot of the probability density of the cosine of the angles between neighboring ethyl groups within a cluster. We calculate the angle between the ethyl groups, which are within the nearest neighbor distance (0.64 nm). We find the probability densities at different concentrations of the water−ethanol binary mixture (black circles are for $x_{eth} \approx 0.05$, red squares are for $x_{eth} \approx 0.10$, blue diamonds are for $x_{eth} \approx 0.15$ and green triangles are for $x_{eth} \approx 0.20$). The solid line is the fit through the data. As expected, the probability density for finding parallel ethyl groups is much higher. However, it is fascinating to note that perpendicular ethyl groups are also probable.

expected the maximum probability appears at ∼2° . It is interesting to note that there is another small peak at ∼85°. This suggests that there are ethanol molecules which are arranged almost perpendicular to each other, as is also evident from the snapshots (Figure 12 and Figure SI4a,b, Supporting Information). This indicates an interesting situation, leading to the competition of the two possible conformations. As we have seen in the case of benzene and several other molecules, existence of two possible conformations leads to strange behaviors. So, this particular aspect of ethanol molecules needs to be explored further. We speculate that the competition between the conformations has been manifested in Figure 5, where the fractal dimension has become arrested after reaching the percolation threshold.

In the aqueous solution of ethanol, the parallel arrangement is expected to be more favorable than that in pure ethanol because of hydrophobic interaction. This is because the potential of mean force between two ethyl groups will be larger in water than that in ethanol. This should lead to efficient packing of the ethanol molecules. This effect should be particularly important at low concentration where the ethanol molecules will form dimers and trimers. The efficient packing of the ethanol molecules explains the excess negative partial volume of the binary mixture.

VI. ENERGY DISTRIBUTION OF ETHANOL MOLECULES: SOUND ABSORPTION COEFFICIENT

In their review Franks and Ives noted, "*Alcohol−water mixtures show excess sound absorption over and above that to be expected from the already excessive absorption coefficients of the pure components. This extra absorption varies greatly from one alcohol to another, depends strongly on the composition of the mixture with water, and decreases rapidly with rising temperature; it must be due to some additional intermolecular relaxation effect.*" In the present work, we looked into the microscopic origin of the excess sound attenuation.

To explain the relevant experimental spectra of sound absorption, Kaatze et al. proposed a unifying model of non-critical concentration fluctuations.[32−34] As discussed in section I, we have found an abrupt increase in local composition fluctuation in the system after $x_{eth} \approx 0.10$, which supports the Kaatze model. The absorption of sound waves, however, demands resonating energy channels to be present in the system. To have an insight into the microscopic origin of these relaxation channels, we calculated the energy distribution of an ethanol molecule in the system at different concentrations. The probability density of the energy of the single ethanol molecules is shown in Figure 7. As the ethanol concentration increases in

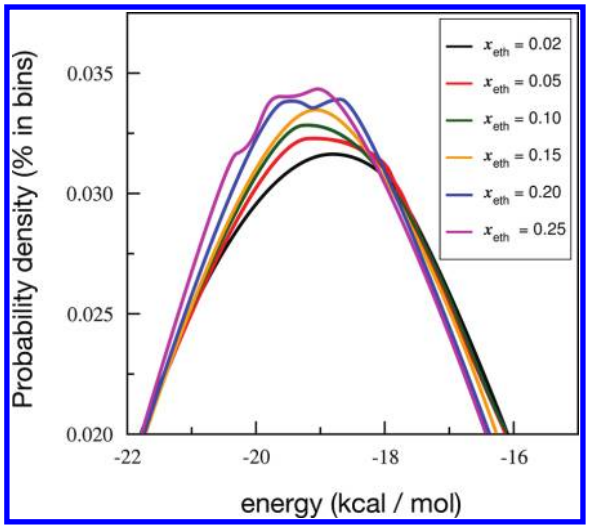

Figure 7. Probability density of the energy of single ethanol molecules in the binary mixture at different concentrations. As noted previously, x_{eth} is the mole fraction of ethanol in the binary mixture. We find that, at $x_{eth} \approx 0.20$, the peak becomes broadened and bifurcated. This interesting nature of the energy distribution indicates additional energy channels for the system, and hence can explain the excess sound attenuation coefficient which reaches the maxima at the same concentration ($x_{eth} \approx 0.20$). It is envisioned that the broadening of the peak occurs due to the difference in environment of the ethanol molecules in the microheterogeneous structure of the binary mixture.

the binary mixture, we find that the peak of the single particle energy distribution becomes broadened, indicating additional energy decay channels that can couple to the sound waves leading to sound attenuation. We presume that the broadening and bifurcation of the peak arises due to the difference in environment of the ethanol molecules in the microheterogeneous structure of the binary mixture. Again, this can be attributed to the orientational ordering among the ethanol molecules due to hydrophobic association.

VII. DRAMATIC COLLAPSE OF A LINEAR HOMOPOLYMER CHAIN AT LOW ETOH CONCENTRATION

There have been growing interests in understanding the behavior of polymer chain immersed in aqueous binary mixture of solvents. Particular attention is being devoted in identifying the change of conformational states along with the change of cosolvent concentration. In an interesting work, Li and Walker[35] measured the monomer solvation free energy of a polystyrene chain in water−ethanol and water−salt mixtures by employing single molecule force spectroscopy. In different

dx.doi.org/10.1021/jp2085439 | J. Phys. Chem. B 2012, 116, 3713−3722

concentrations of those binary mixtures, they found that the polymer − solvent interfacial free energy is directly proportional to the force required to extend the collapsed polymer in a bad solvent. It indirectly implies that the interfacial free energy has a strong dependence on the cosolvent concentration. Previously, in a molecular dynamics study,[36] we have shown that a linear polymer chain (C_n, n = 30−40) prefers the collapsed conformation exclusively in water−DMSO binary mixture at low DMSO concentration ($x_{DMSO} \approx 0.05$).

We take a linear homopolymer of chain length 30 (n = 30, C_{30}) in different concentrations of the water−ethanol binary mixture and observe the conformational change along with the change of the cosolvent concentration. Previous works on such systems suggest that, these hydrophobic groups create an inhomogeneous density distribution in aqueous binary mixtures that contain hydrophobic groups of cosolvents (in this case ethyl group of the cosolvent ethanol), and thus they get preferentially solvated by the cosolvent. The preferential solvation depends on the concentration of the cosolvent as well as length on the polymer chain. The scenario can be potentially interesting at low concentration of ethanol because of the percolation transition predicted here ($x_{eth} \approx 0.06$−0.10). Indeed *we find that at low ethanol concentration the collapsed conformation of the C_{30} polymer gains additional stability, whereas in bulk water it exhibits an interesting bistability between the collapsed and extended conformation* (see Figure 8). As the

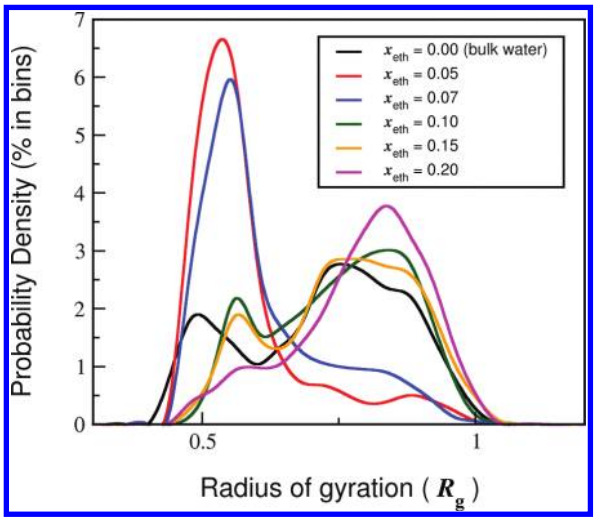

Figure 8. Probability density of the radii of gyration (R_g) of the C_{30} polymer at different ethanol concentrations: (1) $x_{eth} \approx 0.0$ (water), (2) $x_{eth} \approx 0.05$, (3) $x_{eth} \approx 0.07$, (4) $x_{eth} \approx 0.10$, and (5) $x_{eth} \approx 0.20$. As noted previously, x_{eth} is the mole fraction of ethanol in the binary mixture. Clearly the R_g values shows two different states of the polymer − the collapsed state at low R_g and extended state at high R_g. In pure water, the extended state is more stable than the collapsed state of the polymer. We find that the stability of the collapsed state of the polymer increases dramatically at $x_{eth} \approx 0.05$, and decreases subsequently as we gradually increase the concentration of ethanol in the binary mixture.

ethanol concentration is increased gradually this amazing stability of the collapsed conformation starts decreasing, and the polymer stays in both the extended and collapsed conformation for almost equal amount of time. We have computed the radial distribution function of the polymer with respect to the CH_3 groups of ethanol (Figure 9) and it is very much clear

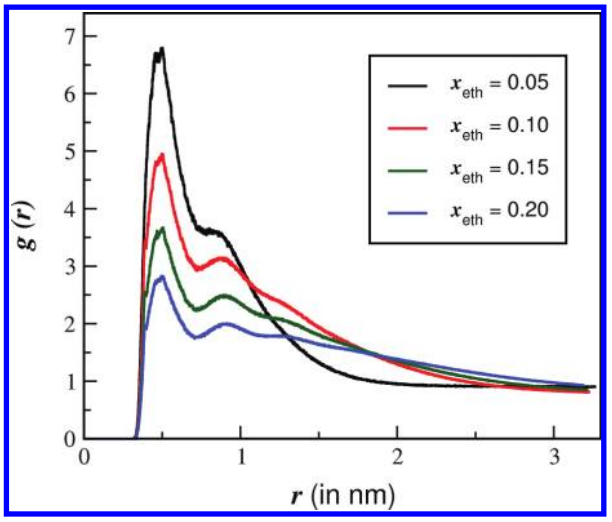

Figure 9. Radial distribution function of the C_{30} polymer with respect to the CH_3 groups of the ethanol. The legend shows the mole fractions of ethanol at different concentrations.

from the plot that at $x_{eth} \approx 0.05$, CH_3 groups of the ethanol molecules comes very close to the polymer, but as the concentration gradually increases, they move away from the same. So it can be concluded that the stabilization of the collapsed state of the polymer at low cosolvent concentration is due to the hydrophobic solvation of the polymer by the hydrophobic part of the ethanol molecules (CH_3−CH_2−).

We follow the fluctuation of radius of gyration (R_g) of the C_{30} polymer in the aqueous ethanol mixture for six different mole fractions of ethanol, $x_{eth} \approx 0.0$(pure water), 0.05, 0.07, 0.10, 0.15, and 0.20 and plot the histograms of probability distributions of R_g (Figure 8). In water, the first and second peaks represent the collapsed and the extended conformations, respectively, and these are of almost equal height. However, at $x_{eth} \approx 0.05$, the first peak makes a steep rise characterizing the remarkable stability of the collapsed conformation. The peak at the extended conformation almost disappears.

At $x_{eth} \approx 0.07$, the height of the first peak decreases a little bit but still the collapsed conformation remains the most stable one. At $x_{eth} \approx 0.10$, the height of the first peak falls sharply as the stability of the collapsed state decreases and extended conformation gains considerable stability. The polymer resides in both the extended and collapsed conformation for almost equal amount of time as is evident from the comparable heights of the two peaks, i.e., the bistability executed in water is regained. The behavior of the polymer remains same also at $x_{eth} \approx 0.15$. At $x_{eth} \approx 0.20$ the extended conformation becomes more stable than the collapsed one as second peak rises above the first one.

The extra-ordinary stability of the collapsed state at low ethanol concentration is attributed to the preferential hydrophobic solvation of the polymer by the hydrophobic part of the ethanol molecules (CH_3−CH_2−). At $x_{eth} \approx 0.05$ an appropriate hydrophobic environment, created around the polymer to effectively solvate the same, stabilizes the collapsed state. In terms of Flory−Huggins theory, this behavior is indicative of a 'bad solvent' for the polymer. In fact, Li and Walker[35] have verified the hypothesis that polymer−solvent interfacial free energy is directly proportional to the force required to extend the collapsed polymer in the solution. They found force plateau

dx.doi.org/10.1021/jp2085439 | J. Phys. Chem. B 2012, 116, 3713−3722

region in water−ethanol mixtures at different concentrations. Their result signifies the coexistence of the extended and collapsed state of the polymer chain in solution, which is in agreement with our simulation results. They also found that with increasing ethanol content, the force plateau decreases, which justify the transition of collapsed−extended coexistence conformation toward fully extended conformation. This also supports our results.

Li and Walker also performed pulling experiments on single polystyrene molecules adsorbed on silicon surface in different aqueous ethanol solvents. They found that, the worse the solvent, the higher was the plateau force and hence higher was the interfacial free energy. They calculated the polystyrene−solvent interfacial free energies by taking the corresponding values from literature[37] and showed the value of the same to be much higher at low ethanol concentration, thereby rationalizing the fact that water−ethanol mixture behaves as a bad solvent at low ethanol concentration. This in turn supports our result of higher stability of collapsed state at low ethanol concentration.

In fact, it has already been reported that ethanol changes the surface tension of water by changing the hydrophobic hydration.[18] That the hydrophobic hydration of ethanol plays a crucial role in polymer collapse can also be understood from the snapshot of the system taken at $x_{eth} \approx 0.05$ (Figure 10).

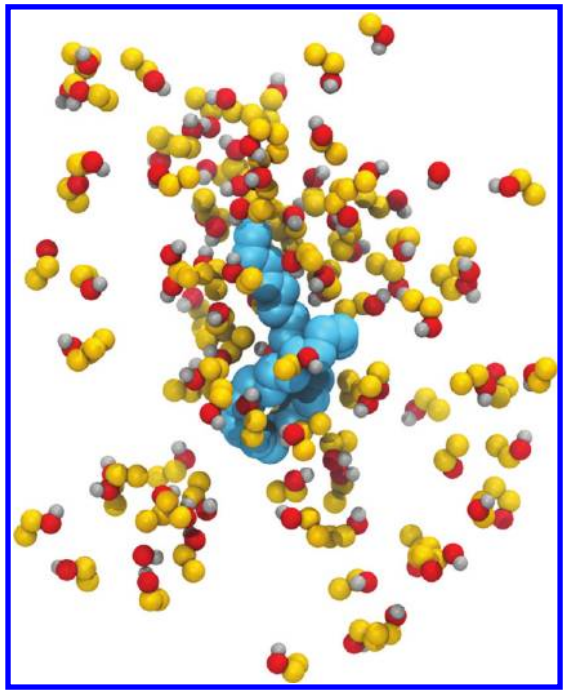

Figure 10. Snapshot of the C_{30} polymer at $x_{eth} \approx 0.05$. The cyan balls are the CH_2 units of the polymer chain, the golden yellow balls are the CH_3 and CH_2 units of the ethanol molecules, the red ones are the oxygen molecules, and silver balls signify the hydrogen molecules.

The snapshot shows the polymer and the ethanol molecules within a distance of 2 nm around the polymer. Here we can clearly see that the ethanol molecules crowd around the polymer at close proximity of the same. However, as the distance from the polymer increases, the crowding gradually starts to decrease and becomes much less dense at the far end. Thus, the polymer induces a local phase separation in the mixture.

We have also calculated the free energy gap between the collapsed and the extended conformation of the C_{30} polymer as a function of the mole fraction of ethanol. This has been plotted in Figure 11). The free energy gap has been calculated from the population analysis according to the formula,

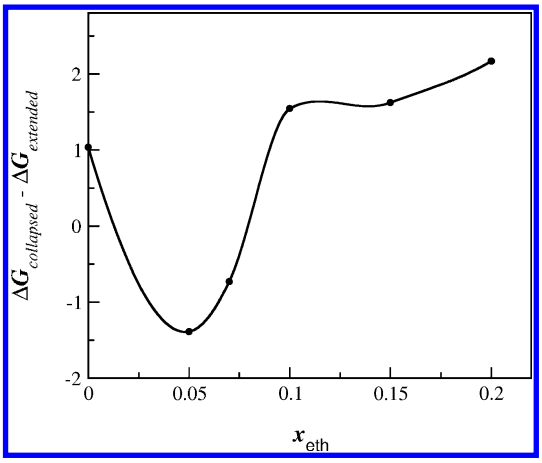

Figure 11. Plot of free energy difference between the collapsed and extended conformation of the C_{30} polymer against mole fraction of ethanol (x_{eth}).

$$\frac{n_{collapsed}}{n_{extended}} = e^{-\Delta(\Delta G)}$$

$$\Rightarrow \Delta(\Delta G) = -\ln\left(\frac{n_{collapsed}}{n_{extended}}\right)$$

$$\text{where, } \Delta(\Delta G) = \Delta G_{Collapsed} - \Delta G_{Extended}$$

Here $\Delta G$is the free energy difference of the conformational state under consideration from a reference state. In this plot we observe that on increasing mole fraction of ethanol from bulk water to $x_{eth} \approx 0.05$, the value of $\Delta G_{collapsed} - \Delta G_{extended}$ drops extensively signifying higher stability of the collapsed conformation at that ethanol concentration. With further increase in ethanol concentration the $\Delta G_{collapsed} - \Delta G_{extended}$ value increases, thereby implying the decreasing stability of the collapsed conformation and emergence of the extended conformation. The value of $\Delta G_{collapsed} - \Delta G_{extended}$ remains almost same for $x_{eth} \approx 0.1$ and 0.15. It again increases at $x_{eth} \approx 0.2$ as the extended conformation gains greater stability.

VIII. CONCLUSION

In order to explore the long known anomalies of water−ethanol binary mixture, we carried out extensive molecular dynamics simulation of this binary mixture at various compositions, with emphasis on low concentration regime where anomalies at low concentration of alcohol solution have long been known but not understood quantitatively. The water−ethanol mixture is of course of particular interest, as this mixture is used in great many applications. Our study revealed that the local composition fluctuation of the system increases abruptly at a concentration, $x_{eth} \approx 0.10$ and it is dependent on the size of the region where the composition fluctuation is determined. The sharp increase in local composition fluctuation indicates a phase-transition-like behavior at that concentration. We also found that the height of the first peak of the radial distribution function of the ethyl groups showed a maximum at $x_{eth} \approx 0.10$.

The most interesting revelation of our study is the evidence of a weak phase transition driven by a percolation transition in

dx.doi.org/10.1021/jp2085439 | J. Phys. Chem. B 2012, 116, 3713−3722

the binary mixture at low ethanol concentration limit. We demonstrated that this picture can explain many anomalies observed in this concentration range of the aqueous alcohol solution. Revisiting the example discussed in the introduction, the marked decrease in the partial molar volume in this concentration limit becomes obvious if the alcohol molecules pack together in an efficient manner, driven by hydrophobicity. The excess sound attenuation coefficient, on the other hand, can be explained by the appearance of additional energy decay channels formed by hydrophobic association. On a similar note, other such anomalies can be explained, although separate studies need to be devoted to quantitatively explain the relationship of the results presented here with the said anomalies.

We applied two distinct methods to detect the percolation threshold. The standard approach of percolation by measuring the moments of the clusters yields the threshold at $x_{eth} \approx 0.06$. On the other hand, a more sophisticated and stable approach involving the fractal dimension[29] yields the threshold at $x_{eth} \approx 0.10$. As discussed previously, we would like to conclude that the percolation transition takes place in this low concentration range, *viz.*, $x_{eth} \approx 0.06-0.10$. Interestingly, this concentration range in mole fraction corresponds to a volume fraction of 17% to 26%. This is an interesting range. It remains as a future exercise to determine the threshold point more accurately by studying a much larger system.

In order to understand the orientation of nearest neighbor ethanol molecules in the binary mixture, we studied the distribution of angle between a central ethyl group and its neighboring ethyl groups. While most of the ethyl groups were found to be in a parallel/antiparallel relative arrangement with each other, some of them were found to be in a perpendicular arrangement!

We have already noted that several other *aqueous* binary mixtures display striking anomalies at low solute concentration. It is interesting to observe that in all these known mixtures that display such anomalous behavior, solute molecules contain both hydrophobic and hydrophilic part. As for example, we have shown recently that in the case of DMSO,[26,27] the anomalies arise due to a percolation-driven transition leading to a bicontinuous phase. In this work also we see that percolation-transition occurs in dilute aqueous ethanol solution. Sokolic et al. have shown similar behavior in water–urea mixture.[38] Though it is too early to comment, yet we think that this percolation transition at low solute concentration of aqueous solution of amphiphiles might be a universal phenomenon.

The most important consequence of the structural transformations observed at relatively low concentrations in these aqueous binary mixtures is the dramatic change in the solvating properties of foreign solutes. We have shown here that the structural transformation induces a dramatic shift in the stability of a polymer chain by making the collapsed conformation considerably more stable. It is known that an aqueous binary mixture at low cosolvent concentration is an important solvent for biological purposes, like in the study of enzymes.[39] We hope to explore these systems in more detail.

IX. METHODS AND SIMULATION

We have performed molecular dynamics (MD) simulation of the water–ethanol binary mixture. All simulations have been done at 300 K temperature and 1 bar pressure. We have used the extended simple point charge model (SPC/E) for water. We have treated the ethanol molecules as united atoms within the GROMOS 53a6 force field, that is, we have retained full atomistic details excepts for the hydrogen atoms attached to the carbon atoms. For the simulation of the polymer we generated an *n*-alkane chain ($n = 30$) and solvated it in a cubic box of water–ethanol solvent. Each side of the cubic box measured 6.654 nm, whereas the maximum length of the polymer could be 4.466 nm in extended configuration. To perform MD simulation, we have used GROMACS (version 4.5.3) which is highly scalable and efficient molecular simulation engine.[40−43]

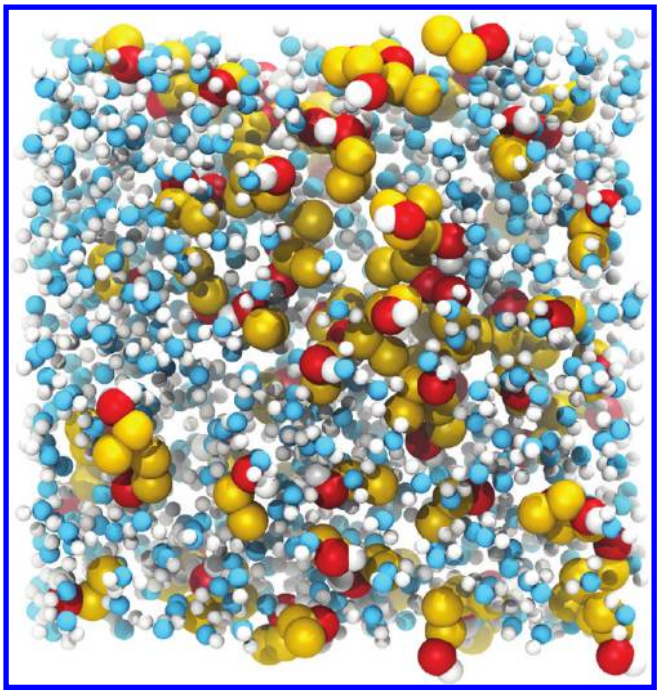

Figure 12. Snapshot of the system at $x_{eth} \approx 0.10$. The golden spheres are the CH_3 and CH_2 groups of ethanol, the red spheres are the O atoms of ethanol, the blue spheres are the O atoms of water, and the white spheres are the H atoms.

We created solvent box containing ethanol and water, performed energy minimization, and then equilibrated them for 2 ns, keeping the volume and temperature constant. After that, we again performed an equilibration at constant pressure and temperature for 2 ns before doing the production run for 20 ns at constant pressure and temperature. The cubic solvent box, in all cases, was approximately 3 nm in length, though there were minor variations in all cases in order to have a proper mole fraction ratio. The calculations of all the properties of the binary mixture were done using these trajectories. Next, we used the equilibrated solvents for solvating the polymer. In this case, the cubic box was 6.654 nm in length. The extended state of the polymer measures 4.466 nm in length. The simulations were carried out for different mole fractions of ethanol.

Periodic boundary condition was applied in all the simulations. We have used Nose–Hoover thermostat for temperature coupling and Parinello–Rahman barostat for pressure coupling. We have used a time step of 2 fs for all the simulations. We employed a grid system for neighbor searching while calculating the nonbonded interactions. Neighbor list generation was performed every 5 step. The cutoff radius for neighbor list and van der Waals interaction was 1.4 nm. To calculate the electrostatic interactions, we used particle mesh Ewald (PME) with a grid spacing of 0.16 nm and an interpolation order of 4.

dx.doi.org/10.1021/jp2085439 | J. Phys. Chem. B 2012, 116, 3713–3722

X. SNAPSHOTS FROM THE SIMULATION

We present some fascinating snapshots of our simulation showing the formation of segregated components in the water−ethanol binary mixture in Figure 12 and in the Supporting Information (Figure SI4). We show the snapshots at three different concentrations, $x_{eth} \approx 0.05$ (Figure SI4a, Supporting Information), $x_{eth} \approx 0.10$ (Figure 11) and $x_{eth} \approx 0.15$ (Figure SI4b, Supporting Information). Even at $x_{eth} \approx 0.05$, we find a tendency of the ethanol molecules to remain close together, but they cannot form a continuous large cluster. Such "infinite" clusters start forming at $x_{eth} \approx 0.10$ and become more prominent at $x_{eth} \approx 0.15$.

■ ASSOCIATED CONTENT

Supporting Information

Plot of $(\sum s^2 n_s)/N_{eth}$ against mole fraction of aqueous ethanol mixture (Figure SI1); sandbox method of calculating fractal dimension (Figure SI2); Free energy surface as obtained from the logarithmic plot of the probability density of the orientation of the ethanol molecules in Figure 6 (Figure SI3); Snapshot of the system at two different concentrations, (a) $x_{eth} \approx 0.05$ and (b) $x_{eth} \approx 0.15$ (Figure SI4). This material is available free of charge via the Internet at http://pubs.acs.org

■ AUTHOR INFORMATION

Corresponding Author

*E-mail: bbagchi@sscu.iisc.ernet.in.

Notes

The authors declare no competing financial interest.

■ ACKNOWLEDGMENTS

We thank Prof. S. Saito for insightful discussions on this problem. We also thank Dr. S. Chakraborty, Dr. B. Jana, Mr. M. Santra, Mr. R. S. Singh, and Mr. R. Biswas for helpful discussions. This work was supported in parts by grants from DST and CSIR, India. B.B. acknowledges support from the J. C. Bose Fellowship.

■ REFERENCES

(1) Franks, F.; Ives, D. J. G. *Q. Rev. Chem. Soc.* **1966**, *20*, 1−44.
(2) Frank, H. S.; Evans, M. W. *J. Chem. Phys.* **1945**, *13*, 507−532.
(3) Lama, R. F.; Lu, B. C. Y. *J. Chem. Eng. Data* **1965**, *10*, 216−219.
(4) Nakanishi, K.; Kato, N.; Maruyama, M. *J. Phys. Chem.* **1967**, *71*, 814−818.
(5) Schott, H. *J. Chem. Eng. Data* **1969**, *14*, 237−239.
(6) McGlashan, M. L.; Williamson, A. G. *J. Chem. Eng. Data* **1976**, *21*, 196−199.
(7) Mizuno, K.; Oda, K.; Maeda, S.; Shindo, Y.; Okumura, A. *J. Phys. Chem.* **1995**, *99*, 3056−3059.
(8) Larkin, J. A. *J. Chem. Thermodyn.* **1975**, *7*, 137−148.
(9) Dixit, S.; Soper, A. K.; Finney, J. L.; Crain, J. *Europhys. Lett.* **2002**, *59*, 377−383.
(10) Finney, J. L.; Bowron, D. T.; Daniel, R. M.; Timmins, P. A.; Roberts, M. A. *Biophys. Chem.* **2003**, *105*, 391−409.
(11) John, L. F.; Bowron, D. T.; Soper, A. K. *J. Phys.: Condens. Matter* **2000**, *12*, A123.
(12) Turner, J.; Soper, A. K. *J. Chem. Phys.* **1994**, *101*, 6116−6125.
(13) Dougan, L.; Bates, S. P.; Hargreaves, R.; Fox, J. P.; Crain, J.; Finney, J. L.; Reat, V.; Soper, A. K. *J. Chem. Phys.* **2004**, *121*, 6456−6462.
(14) Petong, P.; Pottel, R.; Kaatze, U. *J. Phys. Chem. A* **2000**, *104*, 7420−7428.
(15) Wakisaka, A.; Matsuura, K. *J. Mol. Liq.* **2006**, *129*, 25−32.
(16) Dixit, S.; Crain, J.; Poon, W. C. K.; Finney, J. L.; Soper, A. K. *Nature* **2002**, *416*, 829−832.
(17) Wensink, E. J. W.; Hoffmann, A. C.; van Maaren, P. J.; van der Spoel, D. *J. Chem. Phys.* **2003**, *119*, 7308−7317.
(18) Noskov, S. Y.; Lamoureux, G.; Roux, B. *J. Phys. Chem. B* **2005**, *109*, 6705−6713.
(19) Ben-Naim, A. *J. Chem. Phys.* **1977**, *67*, 4884−4890.
(20) Chandra, A.; Bagchi, B. *J. Chem. Phys.* **1991**, *94*, 8367−8377.
(21) Murarka, R. K.; Bagchi, B. *J. Chem. Phys.* **2002**, *117*, 1155−1165.
(22) Srinivas, G.; Mukherjee, A.; Bagchi, B. *J. Chem. Phys.* **2001**, *114*, 6220−6228.
(23) Ludwig, R. *Angew. Chem., Int. Ed.* **2001**, *40*, 1808−1827.
(24) Marques Leite dos Santos, V.; Brady Moreira, F. G.; Longo, R. L. *Chem. Phys. Lett.* **2004**, *390*, 157−161.
(25) Batista da Silva, J. A.; Moreira, F. G. B.; Leite dos Santos, V. M.; Longo, R. L. *Phys. Chem. Chem. Phys.* **2011**, *13*, 6452−6461.
(26) Banerjee, S.; Roy, S.; Bagchi, B. *J. Phys. Chem. B* **2010**, *114*, 12875−12882.
(27) Roy, S.; Banerjee, S.; Biyani, N.; Jana, B.; Bagchi, B. *J. Phys. Chem. B* **2010**, *115*, 685−692.
(28) Stauffer, D. *Phys. Rep.* **1979**, *54*, 1−74.
(29) Oleinikova, A.; Brovchenko, I.; Geiger, A.; Guillot, B. *J. Chem. Phys.* **2002**, *117*, 3296−3304.
(30) Jedlovszky, P.; Brovchenko, I.; Oleinikova, A. *J. Phys. Chem. B* **2007**, *111*, 7603−7609.
(31) Dyczmons, V. *J. Phys. Chem. A* **2004**, *108*, 2080−2086.
(32) Brai, M.; Kaatze, U. *J. Phys. Chem.* **1992**, *96*, 8946−8955.
(33) Rupprecht, A.; Kaatze, U. *J. Phys. Chem. A* **1999**, *103*, 6485−6491.
(34) Kaatze, U. *J. Mol. Liq.* **2009**, *147*, 149−154.
(35) Li, I. T. S.; Walker, G. C. *J. Am. Chem. Soc.* **2010**, *132*, 6530−6540.
(36) Ghosh, R.; Banerjee, S.; Chakrabarty, S.; Bagchi, B. *J. Phys. Chem. B* **2011**, *115*, 7612−7620.
(37) Dann, J. R. *J. Colloid Interface Sci.* **1970**, *32*, 302−320.
(38) Sokolic, F.; Idrissi, A.; Perera, A. *J. Chem. Phys.* **2002**, *116*, 1636−1646.
(39) Klibanov, A. M. *Nature* **2001**, *409*, 241−246.
(40) Berendsen, H. J. C.; van der Spoel, D.; van Drunen, R. *Comput. Phys. Commun.* **1995**, *91*, 43−56.
(41) Hess, B.; Kutzner, C.; van der Spoel, D.; Lindahl, E. *J. Chem. Theory Comput.* **2008**, *4*, 435−447.
(42) Lindahl, E.; Hess, B.; van der Spoel, D. *J. Mol. Model* **2001**, *7*, 306−317.
(43) Van Der Spoel, D.; Lindahl, E.; Hess, B.; Groenhof, G.; Mark, A. E.; Berendsen, H. J. C. *J. Comput. Chem.* **2005**, *26*, 1701−1718.